Environ Earth Sci
DOI 10.1007/s12665-014-3657-z

ORIGINAL ARTICLE

Major ion chemistry, weathering process and water quality of natural waters in the Bosten Lake catchment in an extreme arid region, NW China

Jun Xiao · Zhangdong Jin · Jin Wang · Fei Zhang

Received: 31 October 2013 / Accepted: 21 August 2014

Abstract The concentrations of major ions in the surface water and the groundwater of the Bosten Lake catchment before and during rainy seasons were analyzed to determine the major ion chemistry, geochemical process and to assess the water quality for drinking and irrigation purposes. Natural waters were hard-fresh water with an alkaline nature and a Ca^{2+}–HCO_3^- water type. Although much of physicochemical parameters were under the highest desirable limits set by the Chinese Government for drinking purpose, some samples were not suitable for drinking with reference to the concentrations of NO_3^- and SO_4^{2-}. The sodium adsorption ratio and sodium percentage (%Na) values indicated that most waters were suitable for irrigation. Seasonal variations of ion concentrations and water quality were minor. Saturation index in waters showed that most of the waters were oversaturated with respect to aragonite, calcite, dolomite and magnesite, whereas undersaturated to gypsum and halite. Carbonate weathering and evaporite dissolution were the primary and secondary sources of the dissolved ions, whereas anthropogenic input played a minor role. For the sustainable development of Bosten Lake, a reduction of discharge water from salt washing and an increase in the fresh water inflow to the lake are needed.

Keywords Bosten Lake · Major ion chemistry · Water quality · NW China

J. Xiao (✉) · Z. Jin · J. Wang · F. Zhang
State Key Laboratory of Loess and Quaternary Geology, Institute of Earth Environment, Chinese Academy of Sciences, Xi'an 710075, China
e-mail: xiaojun@ieecas.cn

Introduction

In the arid northwest of China, water resources play a key role in the development of life, agriculture and ecology (Si et al. 2009). Water shortages and poor water quality limit urban development in these areas. The major chemical composition of natural waters can reveal the nature of weathering, patterns and linkages between evaporation and anthropogenic processes on a basin-wide scale (Chetelat et al. 2008; Jin et al. 2009; Xu et al. 2011; Zhang et al. 2011; Xiao et al. 2012a). To effectively utilize and protect water resources in these areas, it is necessary to understand the hydrochemical characteristics and water quality firstly (Tizro and Voudouris 2008; Vetrimurugan et al. 2013; Zhu et al. 2013).

Located in the southern part of Xinjiang, NW China, Bosten Lake is the largest inland freshwater lake in China (Cheng 1995). It is important for grain, melon and fruit, and aquatic product in southern Xinjiang. Due to large-scale agriculture development and irrational water resources utilization in the upper and middle reaches of the Tarim River, the lower Tarim River nearly dried up in 1972, which has brought serous influences to people's life and local ecology (Feng et al. 2005). In 2000, the Chinese Government initiated an environmental restoration project with 10.7 billion Yuan to diverse water from Bosten Lake to the lower reaches of the Tarim River (Fig. 1). Such that, Bosten Lake has served many functions in the region, such as water supply for industry and population, flood control, drought relief, and environmental conservation (Zuo et al. 2006). Previous works in this area have focused on evaluating Holocene climate change (Chen et al. 2006; Huang et al. 2009; Mischke and Wünnemann 2006; Wünnemann et al. 2006), and lake level change (Wang et al. 2003). Despite the importance of natural waters in the BLC, very

Published online: 04 September 2014

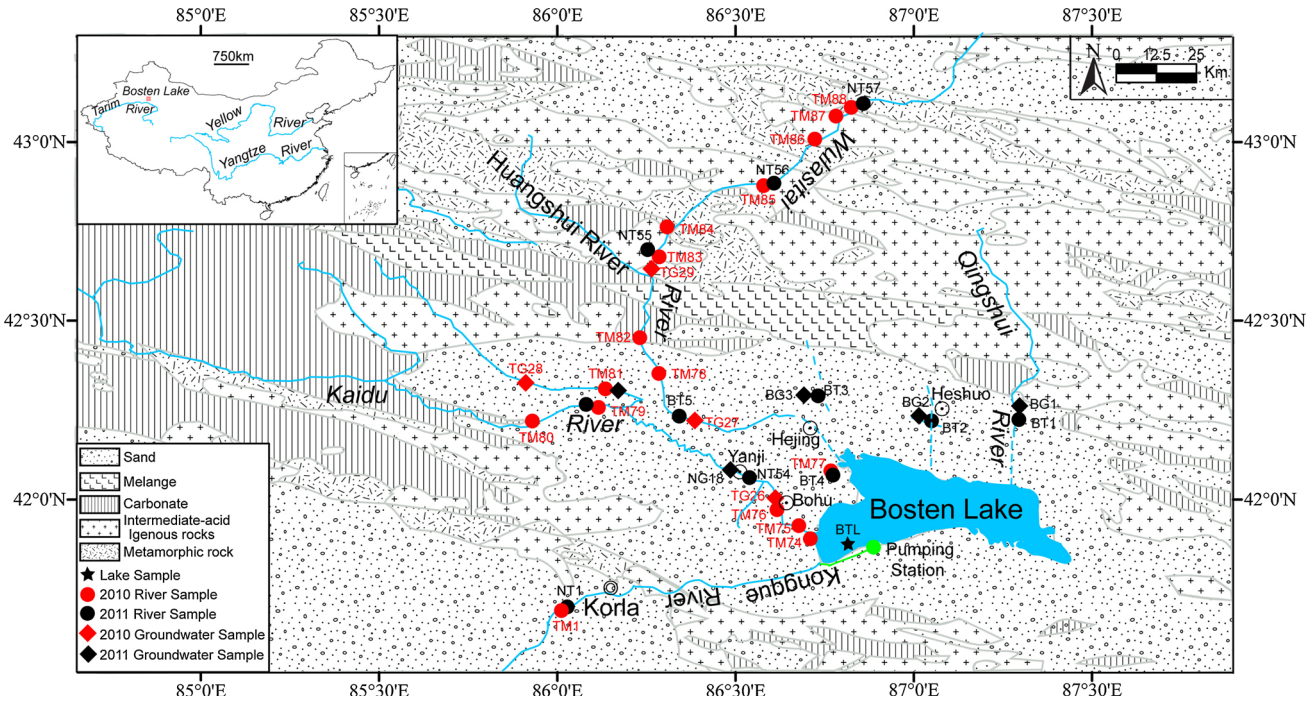

Fig. 1 Sample sites and geology of the study area

little is currently known regarding the water quality and hydrochemical characteristics throughout the catchment.

In the present study, the major ions of 35 water samples in BLC, including 20 river and 15 well waters, were measured to identify geochemistry, quality and solutes sources of natural waters in this area. This knowledge will not only provide a better understanding of the solute geochemistry in arid environments, but will also help the government to develop suitable utilization strategies for the water resources. In addition, it can provide informations for the other similar inland rivers in the world.

Site description and catchment geology

Bosten Lake (86°40′–87°26′E, 41°56′–42°14′N) is located in the southeastern part of Bohu County, Xinjiang (Fig. 1). It fills the intramontane Yanji Basin between the southern slopes of the Tianshan range and the Taklimakan desert. The lake covers a water area of 1,100 km^2, with length about 55 km from east to west and width about 25 km from south to north. The lake surface is 1,048 m above sea level (m.a.s.l.) and the average water depth is 9 m with the maximum depth of 17 m. The total water capacity of the lake is 88 × 10^8 m^3, and the lake water retention time is 4.8 years (Xiao et al. 2010). The BLC is deep-dish shaped, with a quite flat bottom (Cheng 1995).

Bosten Lake receives water from a catchment area covering about 56,000 km^2 with 13 rivers flowing into the lake. It is mainly supplied by a perennial river (Kaidu River), and three intermittent rivers (Huangshui, Wulasitai, and Qingshui Rivers) (Fig. 1), accounting for 96 % of the total annual water input. The Kaidu River is the largest river within the BLC (Chen et al. 2006), with its total length of 513 km, catchment area of 2.2 × 10^4 km^2, and average annual water discharge of 3.412 × 10^9 m^3 (Zuo et al. 2006). About 15 % of the annual Kaidu River runoff originates from meltwater, runoff of which is 10 times larger than other rivers. Intermittent rivers account for 84 % of the total annual runoff (Jin 1990; Wang and Dou 1998). Only about 10 km away from the Kaidu River inflow, the Konque River drains Bosten Lake to flow further south towards the Tarim Basin. Since 1982, the natural outlet of the lake has been replaced by a channel and a pump station to control the water budget of the lake (Fig. 1).

The climate of BLC is a typical arid temperate influenced by the Westerlies. The mean annual air temperature, precipitation and evaporation are about 8.3 °C, 70 and 2,000 mm, respectively (Huang et al. 2009). Rainfall is high in the upper catchment and may exceed 400 mm in the highest ranges of the eastern Tianshan Mountains. The dry climate leads to a vegetation community composed of alpine meadow, steppe, desert steppe and desert with no distinct forest. In addition, some intrazonal vegetation is widely distributed, e.g., small areas of *Picea schrenkiana* forest on the shaded slopes or valleys, some Ulmaceae trees in valleys and some halophyte vegetation on alkaline soil.

It is also notable that a large area of Phragmites and Typha plants grows in the swamp on the western side of Bosten Lake (Huang et al. 2004; Xu et al. 1996). A widespread mobile dune field with complex dunes of up to 100 m height has developed on the pediment plain between Kuruktag and the lake. The dunes partly migrate into the modern water body.

Materials and methods

Twenty water samples were collected on August 18–26, 2010, during the rainy season of the basin; 15 water samples were collected on May 18–26, 2011, during the dry season of the basin (Fig. 1). Water samples were filtered in situ on collection through 0.22 μm Whatman® nylon filters. For cation analysis, a 60-mL aliquot was stored in a pre-cleaned high-density polyethylene (HDPE) bottle and was acidified to pH < 2 with 6 M ultrapure HNO_3. A 30-mL aliquot of the unacidified sample was collected for anion analysis. Then, a strip of Parafilm was slightly stretched and wrapped around the lid of the bottle to ensure no leakage after the outside of the bottle was dried. The electric conductivity (EC), pH, and temperature (T) were determined in situ using portable Orion EC/pH meter at each site. All the samples were stored at 4 °C until analysis. The samples were analyzed for cations (Ca^{2+}, K^+, Mg^{2+}, and Na^+) and Si using a Leeman Labs Profile ICP-OES at Nanjing Institute of Geography and Limnology, Chinese Academy of Sciences (CAS). Repeated analyses demonstrated reproducibility within 2 %. A Dionex-600 ion chromatograph was used for the analysis of F^-, Cl^-, NO_3^-, and SO_4^{2-} at the Institute of Earth Environment, CAS. The average replicated sample reproducibility was 0.5–1 % (2σ). Alkalinity was titrated by Gran titration using 0.1 N HCl within 12 h. Saturation index (SI) of the samples was calculated using the Geochemist's Workbench 8.0 software (Bethke and Yeakel 2009).

Results

Major ion compositions

Chemical compositions and physicochemical parameters of water samples are summarized in Table 1. The pH values ranged from 8.4 to 9.8 in 2010, with an average of 9.4, and from 7.5 to 9.2 in 2011, with an average of 8.4, indicating their alkaline nature. The permissible pH for drinking water varies from 6.5 to 8.5 (Ministry of Health 2006). Outside of these limits, the mucus membranes are affected (Rao et al. 2012). Approximately 80 % of the samples were exceeded the maximum permissible pH. The total dissolved solids (TDS) varied from 41.4 to 3,872 mg/L in 2010, with a mean value of 500 mg/L, and from 57 to 2,939 mg/L in 2011, with a mean value of 606 mg/L. The average TDS values in the BLC were lower than those of the Tarim River (Xiao et al. 2012b), but were higher than those of the rivers in the Lake Qinghai Catchment (Zhang et al. 2009), the Yellow River (Chen et al. 2005), and the Changjiang River (Chetelat et al. 2008). With the exception of TM77 and BT4 (Fig. 1), the waters in the BLC were fresh water with TDS values <1,000 mg/L. In general, TDS values of the Kaidu and Wulasitai Rivers increased from the upper to the lower reaches. The total cationic charge ($TZ^+ = Na^+ + K^+ + 2Mg^{2+} + 2Ca^{2+}$) varied from 0.5 to 61.3 meq/L, with an average of 9.1 meq/L, much higher than the average of world rivers ($TZ^+ = 1.25$ meq/L; Meybeck 1981), and the Changjiang River ($TZ^+ = 2.80$ μeq/L; Han and Liu 2004). The anionic charge ($TZ^- = NO_3^- + F^- + Cl^- + 2SO_4^{2-} + HCO_3^-$) varied from 0.6 to 61.0 meq/L, with an average of 9.2 meq/L. The normalized inorganic charge balance ($NICB\% = 100 \times (TZ^+ - TZ^-)/TZ^+$) varied from −8.0 to 4.6 %, with an average of −0.7 %, indicating the accuracy of our data. The mean concentrations of Ca^{2+}, K^+, Mg^{2+}, Na^+, SiO_2, F^-, Cl^-, NO_3^-, SO_4^{2-}, and HCO_3^- were 1,255, 180, 1,014, 1,988, 211, 11, 1,869, 41, 1,167, and 3,028 μmol/L in 2010, and were 1,614, 142, 1,203, 2,656, 146, 21, 2,140, 78, 1,502, and 3,663 μmol/L in 2011, respectively (Table 1). The major ion concentrations were slightly lower in the rainy season than in the dry season. The relative abundance of major cations and anions were ranked in the order $Na^+ > Ca^{2+} > Mg^{2+} > K^+$ and $HCO_3^- > Cl^- > SO_4^{2-} > NO_3^- > F^-$, respectively. Na^+ and Ca^{2+} together accounted for 59–84 % of the total cations, whereas HCO_3^- and Cl^- for 44–89 % of the total anions.

The correlations between the ions were calculated using SPSS software (Table 2). Strong-positive correlations with significant P levels <0.01 were obtained for Mg^{2+}–Ca^{2+}, Ca^{2+}–Na^+, Mg^{2+}–Na^+, Mg^{2+}–K^+, K^+–Na^+, Ca^{2+}–SO_4^{2-}, Mg^{2+}–SO_4^{2-}, K^+–SO_4^{2-}, Mg^{2+}–Cl^-, Na^+–Cl^-, K^+–Cl^- and Cl^-–SO_4^{2-}, indicating the predominance of chemical weathering along with leaching of secondary salts. The TDS and EC values were primarily correlated with the concentrations of Ca^{2+}, Mg^{2+}, K^+, Na^+, Cl^- and SO_4^{2-} (Table 2).

Water types

Weathering of different parent rocks yields different combinations of dissolved cations and anions. For instance, Na^+ and K^+ are supplied by the weathering of evaporites and silicates, Ca^{2+} and Mg^{2+} by the weathering of carbonates, silicates and evaporites, HCO_3^- by carbonates and silicates, and SO_4^{2-} and Cl^- by evaporites. Silica, on the other hand, is derived exclusively from the weathering of

Table 1 Summary statistics for physicochemical parameters in the BLC and the Chinese State Standard (CSS) for drinking water

Parameters	Year	Minimum	Maximum	Average	SD	CSS
pH	2010	8.4	9.8	9.4	0.5	6.5–8.5
	2011	7.5	9.2	8.4	0.5	
Temperature (°C)	2010	1.4	25.9	13.3	6.4	
	2011	2.6	28.1	20.1	6.4	
TDS (mg/L)	2010	41	3,873	500	802	1,000
	2011	57	2,939	606	664	
EC (μS/cm)	2010	48	5,695	724	1,182	
	2011	66	4,270	880	993	
Ca^{2+} (μmol/L)	2010	185	5,675	1,255	1,073	
	2011	260	4,287	1,614	889	
Mg^{2+} (μmol/L)	2010	36	8,518	1,014	1,783	
	2011	45	7,411	1,203	1,763	
K^{+} (μmol/L)	2010	27	1,854	180	397	
	2011	19	743	142	178	
Na^{+} (μmol/L)	2010	10	29,501	1,988	6,516	8,696
	2011	50	19,876	2,656	4,961	
F^{-} (μmol/L)	2010	8	16	11	2	53
	2011	10	55	21	10	
Cl^{-} (μmol/L)	2010	55	26,554	1,869	5,843	7,042
	2011	82	15,614	2,140	3,869	
SO_4^{2-} (μmol/L)	2010	26	14,063	1,167	3,052	2,604
	2011	98	12,171	1,502	2,961	
NO_3^{-} (μmol/L)	2010	0.5	307	41	66	161
	2011	0	239	78	86	
HCO_3^{-} (μmol/L)	2010	430	6,315	3,028	1,203	
	2011	492	6,377	3,663	1,574	
SiO_2 (μmol/L)	2010	19	587	211	114	
	2011	36	298	146	75	
NICB (%)	2010	−6	11	–0.4	4	
	2011	−6	4	0.01	3	

Table 2 Correlation coefficients between major ions in natural water

	TDS	Ca	Mg	K	Na	HCO_3	Cl	SO_4	F	NO_3	SiO_2	EC
TDS	1	0.94	0.99	0.95	0.99	0.65	0.99	0.99	0.01	0.03	0.60	1
Ca		1	0.91	0.88	0.90	0.81	0.90	0.89	0.08	0.22	0.68	0.93
Mg			1	0.93	0.99	0.59	0.98	0.99	0.01	0.10	0.54	0.99
K				1	0.97	0.52	0.98	0.93	0.01	0.10	0.66	0.95
Na					1	0.55	0.99	0.99	0.03	0.11	0.55	0.99
HCO_3						1	0.54	0.54	0.14	0.49	0.69	0.62
Cl							1	0.98	0.02	0.12	0.59	0.59
SO_4								1	0.01	0.12	0.50	0.99
F									1	0.15	0.10	0.08
NO_3										1	0.25	0.25
SiO_2											1	0.06
EC												1

Correlation is significant at the 0.01 level (2-tailed)

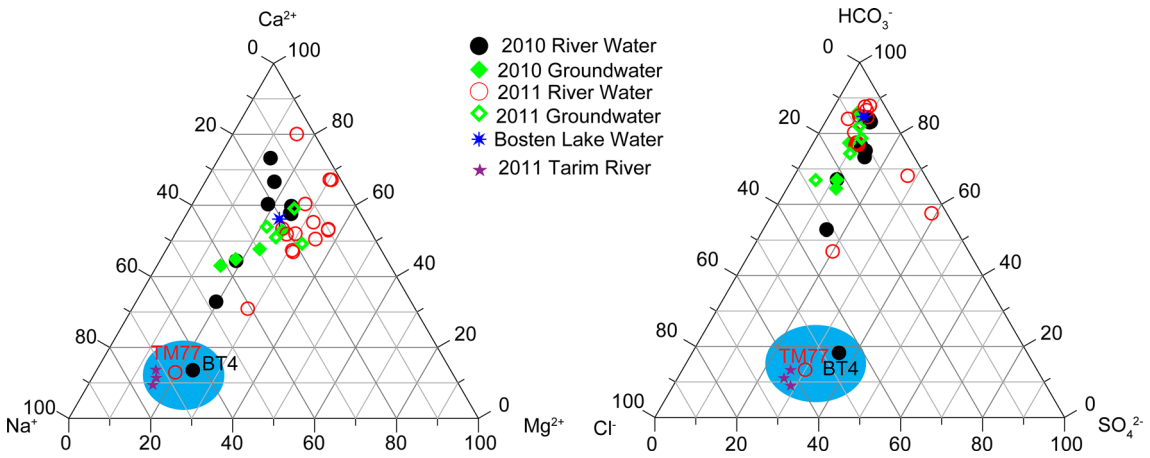

Fig. 2 Ternary diagrams for the cations and anions in waters in the BLC. With the exception of BT4, TM77, and the Tarim River, Ca^{2+} and HCO_3^- dominated in cations and anions with a Ca^{2+}–HCO_3^- water type

silicates, and weathering of carbonates might contribute to the silica fluxes due to the dissolution of biogenic silica in carbonates (Jansen et al. 2010).

To probe the relative importance of different weathering regimes, ternary diagrams of major ion compositions were constructed (Wu et al. 2005). The ternary diagrams showed that nearly all waters have high Ca^{2+} and HCO_3^- concentrations but low Cl^- and Na^+ concentrations, with the exception of BT4 and TM77 (Fig. 2). These samples belonged to the Ca^{2+}–HCO_3^- type, which presumably inherited the chemistry of the underlying carbonate-rich sedimentary rocks in this area (Fig. 1). These samples were basically the same water type with the Aksu River in the Tarim River Basin (Xiao et al. 2012b), the Erlqis and Yili Rivers in northern Xinjiang (Zhu et al. 2011, 2013). For the samples of BT4 and TM77, Na^+ and Cl^- were dominated in the cations and anions, respectively (Fig. 2). The relative abundance of cations and anions were ranked in the order $Na^+ > Ca^{2+} > Mg^{2+} > K^+$ and $Cl^- > HCO_3^- > SO_4^{2-}$, respectively. Both of them belonged to the Na^+–Cl^- type, indicating a contribution of evaporite dissolution. This was the same water type with the Tarim River (Fig. 2) and the rivers in southern Tarim River Basin (Xiao et al. 2012b).

Discussion

Water quality assessment

Drinking water

River water and groundwater in the BLC were primarily used for irrigation and drinking, respectively. TDS versus total hardness (TH) plot (Fig. 3a) showed that 86 % of the samples were hard-fresh water, 8 % of the samples (BT4, TM77 and BTL) were belonged to hard-brackish water, and that NT57 and TM 88 were soft-fresh water. River water quality was slightly better than groundwater (Fig. 3a). With the exception of TM77 and BT4, TH and TDS were within the permissible limits for drinking purpose of 450 and 1,000 mg/L prescribed by the Ministry of Health (2006). Fluoride is essential to prevent dental caries, but excess intake could cause dental/skeleton fluorosis, and further lead to cancer and osteosclerosis (Sun et al. 2011; Rao et al. 2013). High contents of sulfate in drinking water could cause diarrhea, dehydration or weight loss (WHO 2006), whereas high nitrate concentrations could result in birth malformation, hypertension and high-Fe hemoglobin (Carpenter et al. 1998). The maximum allowed concentrations of fluoride, sulfate and nitrate in drinking water are 1.0, 250 and 10 mg/L, respectively (Ministry of Health 2006). Fluorine concentrations of all natural waters were below these limits. Sulfate concentrations in T4 and TM77 and nitrate concentrations in BT2, BG1-3, NG18, and TG28 exceeded their permissible drinking standard, which might be influenced by agricultural fertilizers. Generally, water quality in this area is suitable for drinking.

Bosten Lake is at the confluence of surface water, ground water and farmland discharge water of the Yanqi Basin. Although the river waters in this area were fresh water with low TDS, Bosten Lake water was belonged to very hard brackish water (Fig. 3a). This can be attributed to long-term evaporation and farmland discharge. The cultivated land in the BLC had been increased rapidly since 1959 (Wei 1996). The cultivated area was mostly developed from the edge of the diluvial fan or the delta downstream of the Kaidu River and its alluvial plain. In these areas, the salinity of the waters recharging from these farmlands was very high. Over 40 % of annual salinity discharged into the lake was from farmland discharge

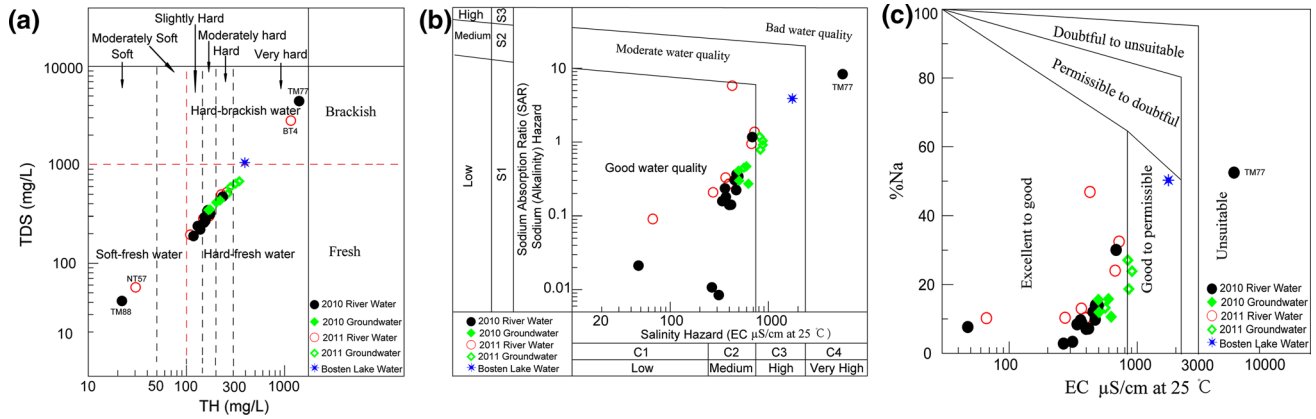

Fig. 3 Natural water quality for drinking (**a**) and irrigation purposes (**b**, **c**) in the BLC

water (Wei 1996). These waters with high salinity increased the salinity of the lake, as one of the main factors for Bosten Lake changing from a fresh lake (before 1970s) to a brackish one. According to TH and TDS limits for drinking purpose in China (Ministry of Health 2006), Bosten Lake is unsuitable for drinking. For the sustainable development of Bosten Lake, a reduction of discharge water from salt washing and/or an increase in the fresh water inflow to the lake are needed.

Irrigation water

The suitable Na^+ concentration in water is important for irrigation, because Na^+ reacts with soil to increase soil hardness and to reduce its permeability. Soil containing a large proportion of sodium with carbonates as the predominant anion, are termed alkali soil; those with chloride or sulfate as the predominant anion are named saline soils. Either type of sodium-saturated soil will support little or no plant growth (Tizro and Voudouris 2008). To identify the availability of the BLC waters for irrigation use, the Wilcox classification diagram based on the EC (μS/cm) and sodium adsorption ratio (SAR) (Wilcox 1955) was employed (Fig. 3b). The SAR directly reflects the degree of Na^+ adsorption by soil and is defined by the following formula (Hem 1991; Rao et al. 2012):

$$\mathrm{SAR} = \mathrm{Na}^+ / \left[\left(\mathrm{Ca}^{2+} + \mathrm{Mg}^{2+}\right)/2\right]^{0.5}$$

where the ionic concentrations were expressed in meq/L. The calculated SAR values of surface water ranged from 0.01 to 7.8, with an average value of 0.9. Groundwater in the rainy season and river waters (except TM77) fell in the C1-S1 and C2-S1 fields (Fig. 3b), indicating low-to-medium salinity and low alkalinity hazards. These samples (83 %) could be used for irrigating most the soils and crops with little danger of exchangeable Na^+ (Raju et al. 2011). Groundwater collected in dry season and the lake water was categorized as C3-S2, indicating high salinity and medium alkalinity hazards. These waters (14 %) with moderate quality could be used to irrigate salt-tolerant and semi-tolerant crops under favorable drainage conditions (Raju et al. 2011). For comparison, water quality in the BLC was better than that in the Tarim River and southeastern Tarim River Basin (Xiao et al. 2012b, 2014). Only TM77 was categorized as C4-S3, showing very high salinity and high alkalinity hazards. TM77 was considered as very poor quality, which cannot be used on soils with restricted drainage, and only appropriate for plants with good salt tolerance (Raju et al. 2011).

To further evaluate water quality for irrigation, the sodium percentage (%Na) was used and calculated using the following equation (Wilcox 1955; Rao et al. 2012; Xiao et al. 2014):

$$\%\mathrm{Na} = \left(\mathrm{Na}^+ + \mathrm{K}^+\right)/\left(\mathrm{Ca}^{2+} + \mathrm{Mg}^{2+} + \mathrm{K}^+ + \mathrm{Na}^+\right) \times 100$$

where all ionic concentrations were expressed in meq/L.

According to the %Na values, water quality could be divided into three groups (Fig. 3c). As shown in Fig. 3b, groundwater collected in 2010 and river waters (except TM77) were categorized as excellent to good; groundwater collected in 2011 and the lake water were categorized as good to permissible; only TM77 fell in the zone of unsuitable (Fig. 3c). Therefore, water in this area is for suitable for irrigation. For the same location, water quality was slightly better in the rainy season than in the dry season, which may be related with the high evaporation in the dry season and strong dilution in the wet season.

Sources of the major components of natural waters

The potential sources of Na^+ and K^+ in natural waters are atmospheric precipitation, evaporite dissolution and the weathering of Na-bearing silicate minerals. Marine

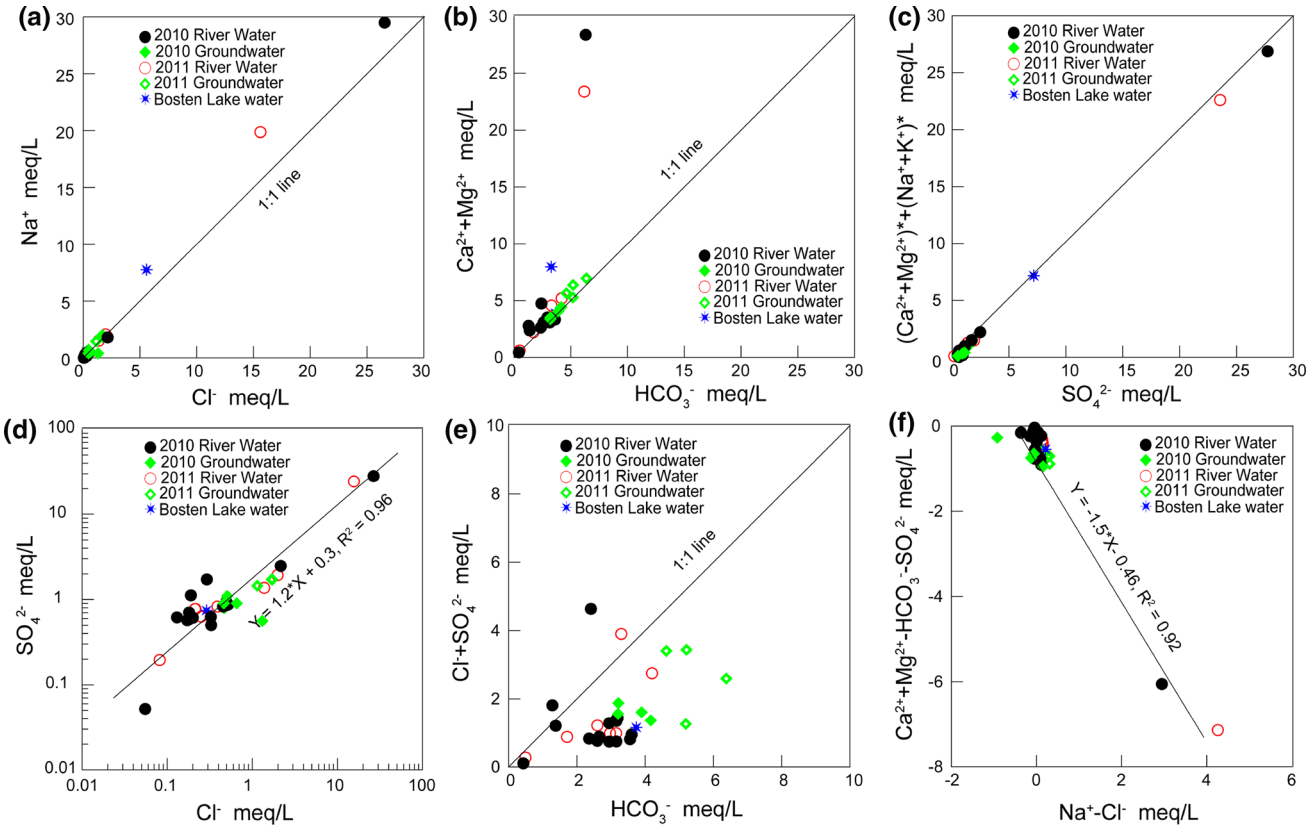

Fig. 4 Ion scatter diagram of waters in the BLC

aerosols and atmospheric dust might contribute Na^+ and Cl^- to natural waters. However, being remote from ocean, contribution of marine aerosols to Na^+ and Cl^- must be minor. If halite dissolution were the source of Na^+, then the Na/Cl molar ratio would be approximately one. In our study, average molar ratio of Na/Cl was 1.04, and most of the samples were close to the 1:1 line (Fig. 4a), indicating the dominance of halite dissolution on water chemistry.

Ca^{2+}, Mg^{2+} and SO_4^{2-} may be from either the weathering of carbonates or the dissolution of evaporates. Under natural conditions (Ca + Mg)/HCO_3 equivalent ratio from carbonate weathering is one. Figure 4b shows that some of the samples were close to the 1:1 line, indicating their source was carbonate weathering. The excess of $(Ca^{2+} + Mg^{2+})$ over HCO_3^- in most of the samples reflected other sources of Ca^{2+} and Mg^{2+}; the excess was balanced by Cl^- and SO_4^{2-}, or an excess of alkalinity was balanced by Na^+ and K^+. The excess of $(Ca^{2+} + Mg^{2+})^*$ over HCO_3^- can be estimated by subtracting HCO_3^- from the total of $(Ca^{2+} + Mg^{2+})$. Similarly, the excess of $(Na^+ + K^+)^*$ over Cl^- can be estimated by subtracting Cl^- from total of $(Na^+ + K^+)$. The $(Ca^{2+} + Mg^{2+})^* + (Na^+ + K^+)^*$ were possibly supplied by sulfate dissolution. Plot of $(Ca + Mg)^* + (Na + K)^*$ versus SO_4^{2-} (Fig. 4c) showed that most of the samples were close to the 1:1 line. In addition, SO_4^{2-} was strongly correlated with Cl^- (Fig. 4d), suggesting a common source for them. These indicated the contribution of the dissolution of sulfate minerals to water solutes. In Fig. 4c, since SO_4^{2-} exceeded $(Ca^{2+} + Mg^{2+})^* + (Na^+ + K^+)^*$, the excess SO_4^{2-} might be from the oxidation of sulfide minerals, e.g., pyrite (Xu and Liu 2010).

Processes controlling major solutes in natural waters within the BLC

Anthropogenic input

The major ion chemistry in natural waters can be affected by human activities. The concentrations of NH_4^+ and $H_2PO_4^-$ mainly reflect the anthropogenic input into the water. However, NH_4^+ and $H_2PO_4^-$ were less than the detection limits in our samples. Thus, anthropogenic source on the water chemistries was minor. In addition, major ion compositions in most samples were within the range of natural water chemistry (Table 2). The low NO_3/Cl (average = 0.1), Cl/Na (average = 0.96), NO_3/Na (average = 0.3), and K/Na (average = 0.6) molar ratios also indicated minor anthropogenic input to the water solute (Chetelat et al. 2008; Liu et al. 2006).

Ion exchange

Ion exchange may be one of the important processes influencing water geochemistry in semiarid/arid areas. Ca^{2+} and Mg^{2+} in waters can be from calcite, dolomite, gypsum and anhydrite and/or cation exchange. The contributions of Ca^{2+} and Mg^{2+} from calcite, dolomite, gypsum and anhydrite dissolution relative to lithologenic Ca^{2+} and Mg^{2+} in waters can be accounted for by subtracting the equivalent concentrations of HCO_3^- and SO_4^{2-}. Similarly, to account for lithologenic Na^+ available for exchange, it is assumed that the Na^+ from meteoric origin would be balanced by an equivalent concentration of Cl^- and, therefore, the equivalent Cl^- concentration is subtracted from that of Na^+. If ion exchange is a significant process, then the relationship between these parameters should be linear with a slope of −1 (Fisher and Mulican 1997). Figure 4f indicates that an increase in Na^+ related to a decrease in $(Ca^{2+} + Mg^{2+})$ or an increase in $(HCO_3^- + SO_4^{2-})$. A negative correlation between $(Ca^{2+} + Mg^{2+} - HCO_3^- - SO_4^{2-})$ and $(Na^+ - Cl^-)$ ($R^2 = 0.92$) suggests the existence of cation exchange of Ca^{2+} and/or Mg^{2+} for Na^+ in waters. The ion exchange is as follows: Na_2–clay + $(Mg^{2+} + Ca^{2+})$ (water) ↔ (Ca + Mg) − clay + $2Na^+$ (water) (Sikdara et al. 2001).

Dissolution and precipitation

Water composition should be balanced or under-/over-saturated with respect to minerals. Dissolution is still ongoing if the water is under-saturated to any mineral, whereas super-saturated water could indicate an ongoing precipitation process. The calculated SI values were ranked in the order dolomite > calcite > aragonite > magnesite > gypsum > halite (Fig. 5). The SI values for aragonite, calcite, dolomite and most magnesite were greater than zero. Thus, waters were oversaturated with respect to these minerals, indicating potential precipitation of secondary calcite, dolomite or magnesite during their transportation into different environments. For example, Bickle et al. (2005) indicated that in some of the Asian mountain waters, up to 70 % of Ca^{2+} derived from carbonate dissolution may be removed during transport from high terrain to lower terrain due to change in water temperature and decreasing concentrations of CO_2. All the SI values for gypsum and halite were less than zero, indicating that they remained under-saturated.

Rock weathering, evaporation and precipitation

In order to assess the functional sources of dissolved chemical constituents, such as rock dominance, precipitation dominance and evaporation dominance, Gibbs diagrams were employed in this study (Gibbs 1970). Gibbs diagrams

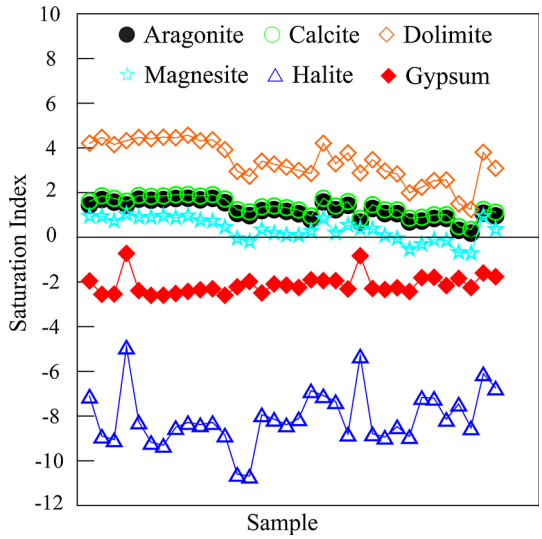

Fig. 5 Saturation index (SI) for calcite, dolomite, aragonite, magnesite, gypsum and halite in water samples in the BLC. Waters were super-saturated with calcite, dolomite, aragonite and most magnesite, but under-saturated with gypsum and halite

of the waters in the BLC, the Tarim River, the Yangtze River and the Yellow River (Chen et al. 2002, 2005; Xiao et al. 2012b) are shown in Fig. 6. TM77 and BT4 with very high TDS values, Na/(Na + Ca) and Cl/(Cl + HCO_3) ratios were plotted on the evaporation zone, indicating the dominant influence of evaporation on the water chemistry. The Bosten Lake water, the Tarim River water (Xiao et al. 2012b) and the Yellow River water (Chen et al. 2005) fell in the junction of evaporation dominance and rock dominance, indicating the influence of both on water chemistry. The other samples, along with the Yangtze River water (Chen et al. 2002), fell in the rock dominance end-member, suggesting their source to be rock weathering.

The $(Cl^- + SO_4^{2-})$ concentrations in most samples were much lower than HCO_3^- (Fig. 4e). The average ratio of HCO_3:(Cl + SO_4):SiO_2 was 21:16:1. In the ternary diagram, Ca^{2+} and HCO_3^- dominated in cation and anion, respectively (Fig. 2). The (Ca + Mg)/(Na + Cl) ratio in most samples were greater than 2. These indicated that carbonate weathering and evaporite dissolution were the primary and secondary sources of the solutes. In addition, there was also no positive relationship between Na^* ($Na^* = Na - Cl$) and SiO_2, indicating that silicate weathering played a less important role in determining major ions.

Quantification of different sources to natural waters

Because the anthropogenic input to water solutes were minor in the BLC, the relative contributions of atmospheric

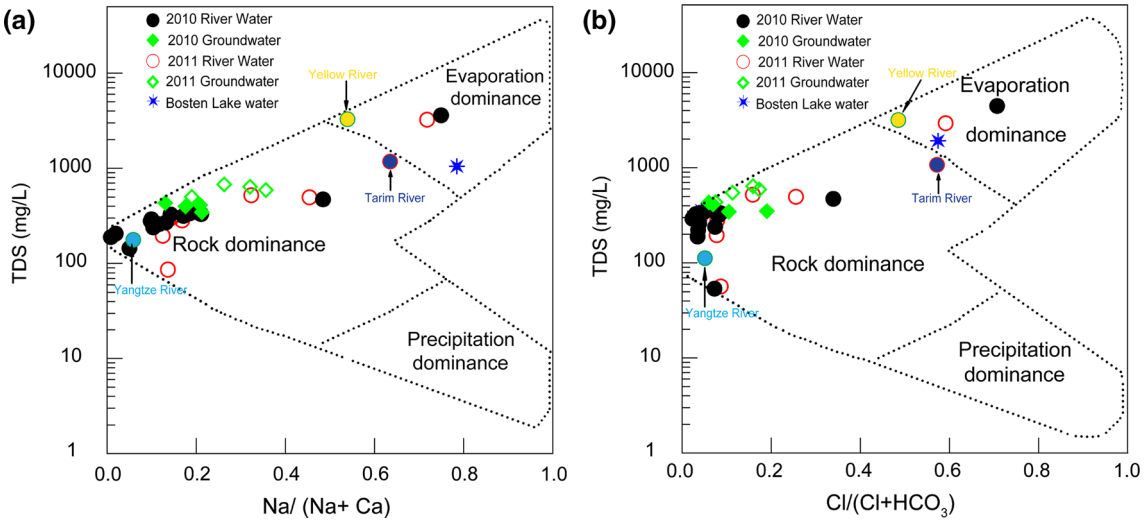

Fig. 6 Gibbs plots of TDS values versus weight ratio of Na/(Na + Ca) (**a**) and Cl/(Cl + HCO_3) (**b**). Most of the samples fell in the water–rock interaction field and only three samples in the evaporation field, suggesting that weathering of rocks primarily controls the major ion chemistry of waters in the BLC

input, carbonate weathering, silicate weathering, and evaporite dissolution were calculated using the forward method (Galy and France-Lanord 1999; Moon et al. 2007). The mass budget equation for any element X in the dissolved load could be written as:

$$[X]_{ws} = [X]_{atm} + [X]_{carb} + [X]_{sil} + [X]_{eva}$$

where ws = water sample; atm = atmospheric input; sil = silicate weathering; carb = carbonate weathering; and eva = evaporite dissolution.

Atmospheric input

Estimation of the atmospheric input is the first step in deciphering the contribution of the different sources of solute at the watershed scale (Chetelat et al. 2008). The lowest Cl^- concentration in TM88 (Cl^-_{min}= 55.1 μmol/L) was assumed to be supplied entirely by atmospheric input. When Cl^- in rainwater is lower than Cl^-_{min}, the corresponding rain component (X_{rain}) was subtracted from the major ion concentrations in samples for correction: $X^*_{ws} = X_{ws} - X_{rain}$, where X_{ws} was the concentration of X in water samples and X^*_{ws} represented the corrected concentration. When Cl^- in rainwater is higher than Cl^-_{min}, the following expressions were used to obtain ion concentrations supplied by rain waters (X^*_{rain}): $X^*_{rain} = X_{rain} \times Cl^-_{min}/Cl_{rain}$; $X^*_{ws} = X_{ws} - X^*_{rain}$. The rainwater data in this study were derived from snow waters collected in the Tianshan Mountain.

The corrected results showed that the proportion of TZ^+ derived from atmospheric input varied from 0.6 to 37.9 % in 2010, with an average of 10.6 %, and from 0.9 to 35.7 % in 2011, with an average of 9.2 %. The atmospheric input showed increased trend upstream in both of the Wulasitai and Kaidu Rivers. On the top of the Tianshan Mountain, atmospheric input could reach to 64 %; whereas, in the lower reaches of the Wulasitai and Kaidu Rivers was ~5 %.

Silicate weathering

The Na^+ in waters was primarily from rainwater, halite dissolution and silicate weathering. To determine silicate contribution to the Na^+ concentration, the corrected Cl^- by atmospheric input was used as an index of evaporite dissolution. If we assumed that all Cl^- was from rainwater and evaporite, the silicate component of Na^+ (Na_{sil}) can be estimated as:

$$Na_{sil} = Na_{ws} - Na_{atm} - Na_{eva}$$

For the silicate component of K^+ (K^+_{sil}), all K^+ was assumed to be of silicate origin, because the evaporites and carbonates had very little K^+. K^+_{sil} might be overestimated due to the existence of sylvites. Since K^+ constituted ~2 % of the total cations in the samples, the uncertainty caused by the above assumption would be very small. The proportions of Ca^{2+} and Mg^{2+} from silicate weathering (Ca^{2+}_{sil} and Mg^{2+}_{sil}) were calculated assuming that they were released to waters from silicates in a fixed proportion relative to Na^+. Thus, the Ca^{2+}_{sil} and Mg^{2+}_{sil} were derived as:

$$Ca^{2+}_{sil} = Na^+_{sil} \times \left(Ca^{2+}/Na^+\right)_{sil}$$
$$Mg^{2+}_{sil} = Na^+_{sil} \times \left(Mg^{2+}/Na^+\right)_{sil}$$

Then, the percentage of the total cation contributions from the silicates to waters, $(\sum Cat)_{sil}$, could be calculated as:

$$\left(\sum Cat\right)_{sil} = TZ^{+}_{sil}/\ TZ^{+}$$

The results indicated that average $(\sum Cat)_{sil}$ was 6.4 % in 2010 and 8.3 % in 2011, respectively. Considering an uncertainty of ±50 % (Galy and France-Lanord 1999; Moon et al. 2007), $(\sum Cat)_{sil}$ varied from 3.2 to 9.6 % in 2010, and from 4.2 to 12.5 % in 2011, respectively.

The ratio of Si to cations can be used as a proxy for the intensity of silicate weathering (Huh et al. 1998). The Si/TZ^{+*} ($TZ^{+*} = TZ^{+} - Cl - 2SO_4$; the evaporite correction) ratio for average shield weathering to kaolinite and gibbsite is 0.78 and 1.6; while for shale weathering to kaolinite and gibbsite is 0.25 and 0.88, respectively (Huh et al. 1998). The Si/TZ^{+*} ratio of our samples varied from 0.02 to 0.15, with an average of 0.07, indicating the shale weathering is the mainly process. Because carbonate weathering is faster than silicates, TZ^{+*} may be dominated by carbonates. To eliminate carbonate and evaporate influence, the ratio of Si to ($Na^{*} + K = Na - Cl + K$) was used (Huh et al. 1998). The Si/($Na^{*} + K$) ratio for weathering of average shield to kaolinite and gibbsite is 1.7 and 3.5, respectively, while for average shale to kaolinite and gibbsite is 1.0 and 3.4, respectively (Huh et al. 1998). The Si/($Na^{*} + K$) ratio of our samples varied from 0.4 to 3.4, with an average of 1.4. The low ratios indicated that the weathering is superficial, i.e., to cation-rich secondary minerals but not to kaolinite and gibbsite.

Carbonate weathering

To calculate the carbonate contribution to waters, Ca^{2+} and Mg^{2+} were assumed to be from atmospheric input, evaporite dissolution, silicate weathering and carbonate weathering. Assuming that all SO_4^{2-} after the correction for atmospheric input was from evaporites, the Ca^{2+} and Mg^{2+} from carbonate weathering, Ca^{2+}_{carb} and Mg^{2+}_{carb}, could be calculated as follows:

$$Ca^{2+}_{carb} = Ca^{2+}_{ws} - Ca^{2+}_{sil} - Ca^{2+}_{eva} - Ca^{2+}_{atm}$$
$$Mg^{2+}_{carb} = Mg^{2+}_{ws} - Mg^{2+}_{sil}$$

Then, the percentage of the total cation contributions from carbonates to waters, $(\sum Cat)_{carb}$, could be calculated as:

$$\left(\sum Cat\right)_{carb} = TZ^{+}_{carb}/TZ^{+}$$

The results indicated that the average $(\sum Cat)_{carb}$ was 54.8 % in 2010 and 48.7 % in 2011, respectively. Because calcite, dolomite and aragonite was super-saturated

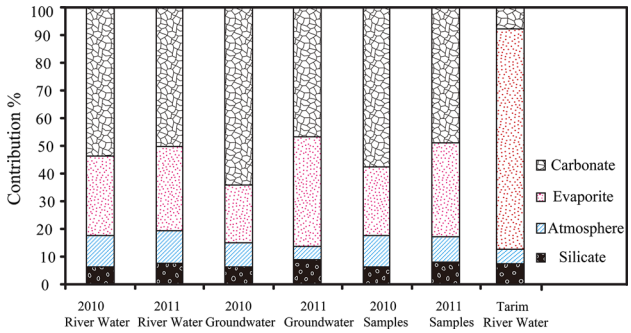

Fig. 7 Calculated contributions (in %) of the different reservoirs to the total cations for the BLC

(Fig. 6), our calculation may thus result in underestimating the carbonate contribution to dissolved cations. Considering an uncertainty of ±50 % (Galy and France-Lanord 1999; Moon et al. 2007), $(\sum Cat)_{carb}$ varied from 27.4 to 82.2 % in 2010, and from 24.4 to 73.1 % in 2011, respectively. The calculation finally provided a contribution from evaporite dissolution, varying from 12.0 to 35.9 % in 2010 and from 16.9 to 50.6 % in 2011.

The relative contributions of different reservoirs to the BLC samples were ranked in the following order: carbonate weathering > evaporite dissolution > atmosphere input > silicate weathering. Compared with the Tarim River waters (Xiao et al. 2012b), carbonate weathering was higher while evaporite dissolution was lower in the BLC (Fig. 7). In addition, seasonal variation of the relative contribution for solutes was minor (Fig. 7). For spatial distribution, evaporite dissolution was stronger around Bosten Lake, whereas carbonate weathering was stronger in the western catchment, in agreement with the distribution of regional lithology in this area (Fig. 1).

TDS flux of the Kaidu River

The Kaidu River is the main tributary and the only largest perennial river of the BLC. The calculated TDS flux of the Kaidu River was 47.4 t/km^2/year, which was only higher than that of the Yellow River (Chen et al. 2005), but lower than that of the Orinoco (Edmond et al. 1996), the Yangtze River (Chen et al. 2002), the Tarim River (Xiao et al. 2012b), the Ganges–Brahmaputra (Galy and France-Lanord 1999), and the Pearl River (Zhang et al. 2007) (Fig. 8). Different from the exorheic rivers in China, the rivers within the BLC are inland rivers, runoff of which finally inflow into Bosten Lake or disappeared in the desert. Under the high evaporation and low precipitation conditions, solutes carried by rivers in this area will increase the soil salinity, and in turn further increase the salinity of river waters or Bosten Lake.

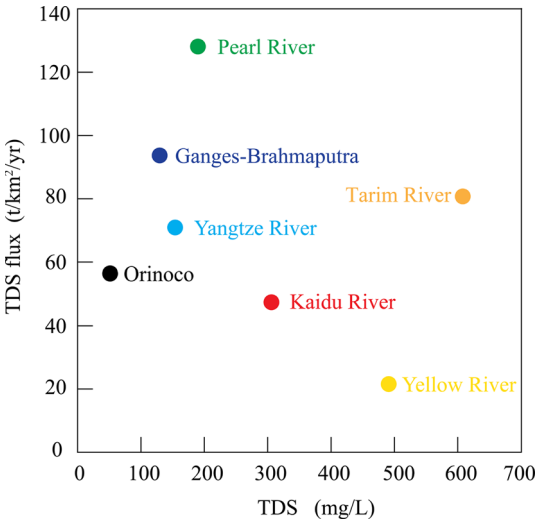

Fig. 8 The relationship of TDS flux with TDS values of the Kaidu River and some of the large rivers in the world. The data of water discharge and area of the Kaidu River were from Zuo et al. (2006)

Conclusions

Natural waters in the BLC were hard-fresh water with an alkaline nature and a Ca^{2+}–HCO_3^- water type. Minor anthropogenic pollution led to good water quality for drinking and irrigation. However, high concentrations of NO_3^- and SO_4^{2-} in some places influenced by agriculture activities should be the focus of future attention. Ion concentrations were slightly lower and water quality was slightly better in the rainy season than in the dry season. Carbonate weathering and evaporite dissolution were the dominant hydro-geochemical processes controlling the solutes in natural waters, but cation exchange and precipitation also played an important role. Evaporite dissolution was stronger around Bosten Lake, whereas carbonate weathering was stronger in the western catchment. The TDS flux of the Kaidu River was 47.4 t/km^2/year, higher than that of the Yellow River, but lower than that of the Yangtze River, the Tarim River, and the Pearl River in China. Our study can lead to an improved understanding for sustainable development of water resources in this area and for hydrochemical systems in other inland rivers in the world.

Acknowledgments This work was financially supported by the "Western Doctor" of the West Light Foundation of CAS, National Science Foundation of China (Grant 41003012 and 41403111) and the Key Research Program of the Chinese Academy of Sciences (Grant KZZD-EW-04-02). We thank Yuxin Zhu of Nanjing Institute of Geography and Limnology, CAS, for his kind help to sample analyses.

References

Bethke CM, Yeakel S (2009) The Geochemist's Workbench®, Version 8.0. Hydrogeology Program. University of Illinois, Urbana, 84 p

Bickle MJ, Chapman HJ, Bunbury J, Harris NB, Fairchild W, Ahmed T, Pomies C (2005) Relative contribution of silicate and carbonate rocks to riverine Sr fluxes in the headwaters of the Ganges. Geochim Cosmochim Acta 69:2221–2240

Carpenter SR, Caraco NF, Correll DL, Howarth RW, Sharpley AN, Smith VH (1998) Non-point pollution of surface waters with phosphorus and nitrogen. Ecol Appl 8:559–568

Chen JS, Wang FY, Xia XH, Zhang LT (2002) Major element chemistry of the Changjiang (Yangtze River). Chem Geol 187:231–255

Chen JS, Wang FY, Meybeck M, He DW, Xia XH, Zhang LT (2005) Spatial and temporal analysis of water chemistry records (1958–2000) in the Huanghe (Yellow River) Basin. Glob Biogeochem Cycles 19:GB3016. doi:10.1029/2004GB00232

Chen FH, Huang XZ, Zhang JW, Holmes JA, Chen JH (2006) Humid little ice age in arid central Asia documented by Bosten Lake, Xinjiang, China. Sci China (Ser D: Earth Sci) 49(12):1280–1290

Cheng QC (1995) Research on Bosten Lake. Hehai University Press, Nanjing, pp 1–7 (in Chinese)

Chetelat B, Liu CQ, Zhao ZQ, Wang QL, Li SL, Li J, Wang BL (2008) Geochemistry of the dissolved load of the Changjiang Basin Rivers: anthropogenic impacts and chemical weathering. Geochim Cosmochim Acta 72:4254–4277

Edmond JM, Palmer MR, Measures CI, Brown ET, Huh Y (1996) Fluvial geochemistry of the eastern slope of the northeastern Andes and its foredeep in the drainage of the Orinoco in Colombia and Venezuela. Geochim Cosmochim Acta 60:2949–2976

Feng Q, Liu W, Si JH, Su YH, Zhang YW, Cang ZQ, Xi HY (2005) Environmental effects of water resources development and use in the Tarim River Basin of northwestern China. Environ Geol 48:202–210

Fisher RS, Mulican WF III (1997) Hydrochemical evolution of sodium-sulphate and sodium-chloride groundwater beneath the Northern Chihuahuan desert Trans-Pecos, Texas, USA. Hydrogeol J 10:455–474

Galy A, France-Lanord C (1999) Weathering processes in the Ganges-Brahmaputra Basin and the riverine alkalinity budget. Chem Geol 159:31–60

Gibbs RJ (1970) Mechanisms controlling world water chemistry. Science 170:795–840

Han GL, Liu CQ (2004) Water geochemistry controlled by carbonate dissolution: a study of the river waters draining karst-dominated terrain, Guizhou Province, China. Chem Geol 204:1–21

Hem JD (1991) Study and interpretation of the chemical characteristics of natural water. United States Geological Survey Water-Supply Paper 2254

Huang XZ, Zhao Y, Cheng B, Chen FH, Xu JR (2004) Modern pollen analysis of the surface sediments from the Bosten Lake, Xinjiang, China. J Glaciol Geocryol 26:602–609 (in Chinese)

Huang XZ, Chen FH, Fan YX, Yang ML (2009) Dry late-glacial and early Holocene climate in arid central Asia indicated by lithological and palynological evidence from Bosten Lake, China. Quatern Int 194:19–27

Huh Y, Panteleyev G, Babich D, Zaitsev A, Edmond JM (1998) The fluvial geochemistry of the rivers of Eastern Siberia:II. Tributaries of the Lena, Omoloy, Yana Indigirka, Kolyma, and Anadyr draining the collisional/accretionary zone of the Verkhoyansk and Cherskiy ranges. Geochim Cosmochim Acta 62:2053–2075

Jansen N, Hartmann J, Lauerwald R, Dürr HH, Kempe S, Loos S, Middelkoop H (2010) Dissolved silica mobilization in the conterminous USA. Chem Geol 270:90–109

Jin XC (1990) Eutrophication of Chinese Lakes. Chinese Environmental Science Press, Beijing, p 614

Jin ZD, Yu JM, Wang SM, Zhang F, Shi YW, You CF (2009) Constraints on water chemistry by chemical weathering in the

Lake Qinghai catchment, northeastern Tibetan Plateau (China): Clues from Sr and its isotopic geochemistry. Hydrogeol J 17:2037–2048

Liu CQ, Li SL, Lang YC, Xiao HY (2006) Using $\delta^{15}N$ and $\delta^{18}O$ values to identify nitrate sources in karst groundwater, Guiyang, Southwest China. Environ Sci Technol 40:6928–6933

Meybeck M (1981) Pathways of major elements from land to ocean through rivers. In: Martin JM, Burton JD, Eisma D (eds) River Inputs to Ocean Systems. United Nations Press, New York, pp 18–30

Ministry of Health (2006) Standards for drinking water quality. GB5749-2006. Ministry of Health of the People's Republic of China, Beijing

Mischke S, Wünnemann B (2006) The Holocene salinity history of Bosten Lake (Xinjiang, China) inferred from ostracod species assemblages and shell chemistry: Possible palaeoclimatic implications. Quatern Int (154–155):100–112

Moon S, Huh Y, Qin JH, Pho NV (2007) Chemical weathering in the Hong (Red) River Basin: rates of silicate weathering and their controlling factors. Geochim Cosmochim Acta 71:1411–1430

Raju NJ, Shukla UK, Ram P (2011) Hydrogeochemistry for the assessment of groundwater quality in Varanasi: a fast-urbanizing center in Uttar Pradesh, India. Environ Monit Assess 173:279–300

Rao NS, Subrahmanyam A, Kumar SR, Srinivasulu N, Rao GB, Rao PS, Reddy GV (2012) Geochemistry and quality of groundwater of Gummanampadu Sub-basin, Guntur District, Andhra Pradesh, India. Environ Earth Sci 67:1451–1471

Rao NS, Subrahmanyam A, Rao GB (2013) Fluoride-bearing groundwater in Gummanampadu Sub-basin, Guntur District, Andhra Pradesh, India. Environ Earth Sci 70:575–586

Si JH, Feng Q, Wen XH, Su YH, Xi HY, Chang ZQ (2009) Major ion chemistry of groundwater in the extreme arid region northwest China. Environ Geol 57:1079–1087

Sikdara PK, Sarkar SS, Palchoudhury S (2001) Geochemical evolution of groundwater in the Quaternary aquifer of Calcutta and Howrah, India. J Asian Earth Sci 19:579–594

Sun YB, Fang QH, Dong JP, Cheng XW, Xu JQ (2011) Removal of fluoride from drinking water by natural stilbite zeolite modified with Fe(III). Desalination 277:121–127

Tizro AT, Voudouris KS (2008) Groundwater quality in the semi-arid region of the Chahardouly Basin, West Iran. Hydrol Process 22:3066–3078

Vetrimurugan E, Elango L, Rajmohan N (2013) Sources of contaminants and groundwater quality in the coastal part of a river delta. Int J Environ Sci Technol 10:473–486

Wang SM, Dou HS (1998) Chinese lakes. Science Press, Beijing 580

Wang R, Giese E, Gao QZ (2003) The recent change of water level in the Bosten Lake and analysis of its causes. J Glaciol Geocryol 25:60–64 (in Chinese)

Wei ZY (1996) Surface water chemical changes due to human activities in the Tarim Basin. Geochem J 40:25–29

WHO (2006) Guidelines for drinking-water quality, Recommendations, 3rd edn, vol 1. World Health Organization, Geneva

Wilcox LV (1955) Classification and use of the irrigation waters. US Department of Agriculture Circular No 969, District of Columbia, Washington, p 19

Wu LL, Huh YS, Qin JH, Du G, van Der Lee S (2005) Chemical weathering in the Upper Huang He (Yellow River) draining the eastern Qinghai-Tibet Plateau. Geochim Cosmochim Acta 69:5279–5294

Wünnemann B, Mischke S, Chen FH (2006) A Holocene sedimentary record from Bosten Lake, China. Palaeogeogr Palaeocl 234:223–238

Xiao M, Wu FC, Liao HQ, Li W, Lee XQ, Huang RS (2010) Characteristics and distribution of low molecular weight organic acids in the sediment pore waters in Bosten Lake, China. J Environ Sci 22:328–337

Xiao J, Jin ZD, Zhang F, Wang J (2012a) Solute geochemistry and its sources of the groundwaters in the Qinghai Lake catchment, NW China. J Asian Earth Sci 52:21–30

Xiao J, Jin ZD, Ding H, Wang J, Zhang F (2012b) Geochemistry and solute sources of surface waters of the Tarim River Basin in the extreme arid region, NW Tibetan Plateau. J Asian Earth Sci 54–55:162–173

Xiao J, Jin ZD, Wang J (2014) Geochemistry of trace elements and water quality assessment of natural water within the Tarim River Basin in the extreme arid region, NW China. J Geochem Explor 136:118–126

Xu ZF, Liu CQ (2010) Water geochemistry of the Xijiang Basin rivers, South China: Chemical weathering and CO_2 consumption. Appl Geochem 25:1603–1614

Xu YQ, Yan S, Jia BQ, Yang YL (1996) Numerical relationship between the surface spore-pollen and surrounding vegetation on the southern slope of Tianshan Mountains. Arid Land Geogr 19:24–30 (in Chinese)

Xu ZF, Shi C, Tang Y, Han HY (2011) Chemical and strontium isotopic compositions of the Hanjiang Basin Rivers in China: anthropogenic impacts and chemical weathering. Aquat Geochem 17:243–264

Zhang SR, Lu XX, Higgitt DL, Chen CTA, Sun HG, Han JT (2007) Water chemistry of the Zhujiang (Pearl River): natural processes and anthropogenic influences. J Geophys Res 112:F01011. doi:10.1029/2006JF000493

Zhang F, Jin ZD, Hu G, Li FC, Shi YW (2009) Seasonally chemical weathering and CO_2 consumption flux of Qinghai Lake river system in the northeastern Tibetan Plateau. Environ Earth Sci 59:297–313

Zhang L, Song XF, Xia J, Yuan RQ, Zhang YY, Liu X, Han DM (2011) Major element chemistry of the Huai River Basin, China. Appl Geochem 26:293–300

Zhu BQ, Yang XP, Rioual P, Qin XG, Liu ZT, Xiong HG, Yu JJ (2011) Hydrogeochemistry of three watersheds (the Erlqis, Zhungarer and Yili) in northern Xinjiang, NW China. Appl Geochem 26:1535–1548

Zhu B, Yu J, Qin X, Rioual P, Jiang F, Liu Z, Mu Y, Li H, Ren X, Xiong H (2013) Identification of rock weathering and environmental control in arid catchments (Northern Xinjiang) of Central Asia. J Asian Earth Sci 66:277–294

Zuo QT, Dou M, Chen X, Zhou KF (2006) Physically-based model for studying the salinization of Bosten Lake in China. Hydrol Sci J 51(3):432–449